The Long Terminal Repeat-Containing Retrotransposon Tf1 Possesses Amino Acids in Gag That Regulate Nuclear Localization and Particle Formation

Min-Kyung Kim, Kathryn C. Claiborn,† and Henry L. Levin*

Section on Eukaryotic Transposable Elements, Laboratory of Gene Regulation and Development, National Institute of Child Health and Human Development, National Institutes of Health, Bethesda, Maryland 20892

Tf1 is a long terminal repeat-containing retrotransposon of *Schizosaccharomyces pombe* that is studied to further our understanding of retrovirus propagation. One important application is to examine Tf1 as a model for how human immunodeficiency virus type 1 proteins enter the nucleus. The accumulation of Tf1 Gag in the nucleus requires an N-terminal nuclear localization signal (NLS) and the nuclear pore factor Nup124p. Here, we report that NLS activity is regulated by adjacent residues. Five mutant transposons were made, each with sequential tracts of four amino acids in Gag replaced by alanines. All five versions of Tf1 transposed with frequencies that were significantly lower than that of the wild type. Although all five made normal amounts of Gag, two of the mutations did not make cDNA, indicating that Gag contributed to reverse transcription. The localization of the Gag in the nucleus was significantly reduced by mutations A1, A2, and A3. These results identified residues in Gag that contribute to the function of the NLS. The Gags of A4 and A5 localized within the nucleus but exhibited severe defects in the formation of virus-like particles. Of particular interest was that the mutations in Gag-A4 and Gag-A5 caused their nuclear localization to become independent of Nup124p. These results suggested that Nup124p was only required for import of Tf1 Gag because of its extensive multimerization.

The import of proteins across the nuclear envelope occurs through the nuclear pore complex (NPC), a structure composed of over 30 different factors known as nucleoporins (27). The family of soluble transport receptors termed importins or karyopherins promotes translocation through the NPC by binding to nuclear localization signals (NLSs) present in cargo proteins (14, 32). Translocation occurs when the receptor bound to the cargo associates with arrays of FG repeats present in a family of proteins in the NPC (14, 37). Although the factors that mediate transport into the nucleus have been studied extensively, less is known about how the NPC accommodates very large cargos. Import experiments using gold particles or human hepatitis B virus indicate that the nuclear pore has the capacity to translocate substrates that are significantly larger than the diameter of the pore (24). The processes responsible for this type of import are unknown.

The integrase and cDNA of retroviruses form a large preintegration complex (PIC) that in some cases translocates through the NPC. Because human immunodeficiency virus type 1 (HIV-1) can infect nondividing cells, this PIC must be capable of entering the nucleus through the NPC. The matrix protein, virus protein R, and integrase (IN) protein, as well as the DNA flap structure of the viral cDNA, are components suggested to contribute to nuclear import (8, 11). However,

HIV-1 virions that lack matrix protein or virus protein R can enter the nucleus, indicating that the role of these proteins in nuclear import is unclear (13). In addition to its ability to traffic through the NPC of nondividing cells, the PIC of HIV-1 can also be imported into the nucleus of dividing cells while the nuclear envelope is intact (17). This result underscores the possibility that mechanisms of nuclear import may be important for the propagation of other retroviruses. An example of an unconventional retrovirus that has the ability to be transported into the nucleus is the human foamy virus. The Gag of this virus has C-terminal domains with nuclear localization activity (38).

Long terminal repeat (LTR)-containing retrotransposons are close relatives of retroviruses that share similar structures and mechanisms of propagation with their viral counterparts. The similarities in replication include the sequential steps of particle formation, reverse transcription, and integration. As a result, LTR-containing retrotransposons are important models for the study of retroviruses. One such transposon is Tf1, a functional LTR-containing retrotransposon of *Schizosaccharomyces pombe* that encodes active forms of Gag, protease (PR), reverse transcriptase (RT), and IN (4, 5, 20, 34).

In an effort to model the import of large complexes such as the PIC of HIV-1, the nuclear import of Tf1 in *S. pombe* has been examined. Previous studies identified an NLS in the N terminus of Gag that is required for transposition (10). Mutations in the NLS in the context of the transposon caused a severe defect in the nuclear localization of Gag and the cDNA. In separate experiments, a factor of the nuclear pore, Nup124p, was found to be required for transposition of Tf1 (6). Mutations in *nup124* caused a significant defect in the

* Corresponding author. Mailing address: Section on Eukaryotic Transposable Elements, Laboratory of Gene Regulation and Development, National Institute of Child Health and Human Development, National Institutes of Health, Bethesda, MD 20892. Phone: (301) 402-4281. Fax: (301) 496-4491. E-mail: Henry_Levin@nih.gov.

† Present address: University of Pennsylvania School of Medicine, Philadelphia, Pa.
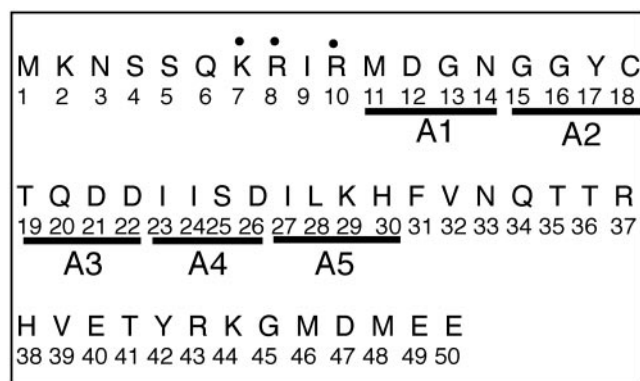
FIG. 1. The five alanine mutations introduced in Gag. Five versions of Tf1 were generated each with a stretch of four amino acids in Gag changed to alanines. The mutations were made in the 20 residues after the N-terminal NLS of Gag. The key residues of the NLS are indicated by dots. The alanine mutations were named A1, A2, A3, A4, and A5. The positions in Gag of the residues changed to alanine are shown above the heavy lines labeled with the name of the mutant.

import of Tf1 Gag. Surprisingly, these mutations did not reduce the import of other proteins. The results of two-hybrid analyses and binding studies revealed a direct interaction between the N terminus of Nup124p and the Gag of Tf1 (6). It was proposed that the binding of Gag to Nup124p could mediate the nuclear import of Tf1.

The function of Nup124p in the import of Tf1 Gag was explored further by studying the import of large proteins consisting of sections of Gag fused to green fluorescent protein (GFP) and LacZ (10). Interestingly, Nup124p was required for import of the first 50 amino acids of Gag fused to GFP-LacZ. However, when specific segments of Gag were removed from this fusion, the protein still localized in the nucleus but the requirement for Nup124p was lost. The requirement for Nup124p was mapped to residues 20 through 30 of Gag.

To identify the region of Gag that confers Nup124p dependence on nuclear localization, we introduced five tracts of four alanine mutations in Gag residues 11 through 30 (Fig. 1). The localization of Gag by indirect immunofluorescence revealed that the Gags of mutations A1, A2, and A3 were not imported into the nucleus. It was interesting that the localization of Gag for A4 and A5 occurred in the nucleus, but the inhibition of import associated with log-phase growth was absent. It was particularly interesting that the import of Gag with the A4 and A5 mutations was not dependent on Nup124p. The mutation in A5 also resulted in a severe defect in particle formation. The results indicate that the 20 residues adjacent to the NLS contained information that regulated nuclear localization of Gag. In addition, the dependence on Nup124p for import corresponded to the ability of Gag to form particles.

MATERIALS AND METHODS

Strains and media. The yeast strains used in this study are listed in Table 1. The media for *S. pombe*, Edinburgh minimal medium (EMM) or yeast extract supplements (YES), were prepared as described previously (19, 23). The EMM was supplemented with dropout powder that lacked uracil but contained all amino acids, each at a concentration of 100 μg/ml, with adenine at 250 μg/ml. The overexpression of Tf1 was achieved by fusing the element to the *nmt1* promoter. Growth in the absence of thiamine (vitamin B1) induced the *nmt1* promoter, while the addition of 10 μM repressed it. For the transposition assay, 1 mg/ml 5-fluoroorotic acid (5-FOA) and/or 500 μg/ml of Geneticin (Invitrogen) was added to the appropriate media.

Plasmid constructions. The oligonucleotides used in plasmid constructions are listed in Table 2, and the plasmids in this study are listed in Table 3. A series of five mutations were made in the Gag of Tf1 in the expression plasmid pHL449-1. Stretches of four amino acid residues from positions 11 to 30 were each replaced by four alanine residues using the method of fusion PCR (18). Briefly, two PCR products (half-products) were produced that overlap at the site of the desired mutation. The nucleotide changes were encoded in the primers used to generate the half-products. Thus, the first round of PCR generated half-products with termini that contained the replaced sequences of Gag. The two half-fragments generated from the first round of PCRs overlapped by about 30 nucleotides where the mutations were made. The two half-products are used as templates in a second PCR that generated a single fragment with the modified sequence. The primers for this reaction contained XhoI and AvrII sites that were used to insert the new fragments into pHL449-1. The oligonucleotides used for fusion PCR are listed in Table 2.

TABLE 1. Strains

Strain	Genotype	Strain or plasmid	Reference or source
YHL 912	*h⁻ ura4-294 leu1-32*	Parent/no plasmid	
YHL1032	*h⁻ ura4-294 leu1-32*	912/pFL20	6
YHL1282	*h⁻ ura4-294 leu1-32*	912/pHL449-1	18
YHL1554	*h⁻ ura4-294 leu1-32*	912/pHL476-3	18
YHL1836	*h⁻ ura4-294 leu1-32*	912/pHL490-80	5
YHL5750	*h⁻ ura4-294 leu1-32 nup124-1*	No plasmid	6
YHL5754	*h⁻ ura4-294 leu1-32 nup124-1*	5750/pHL449-1	6
YHL6773	*h⁻ ura4-294 leu1-32*	912/pHL1757	10
YHL8121	*h⁻ ura4-294 leu1-32*	912/pHL2276	This study
YHL8122	*h⁻ ura4-294 leu1-32*	912/pHL2276	This study
YHL8123	*h⁻ ura4-294 leu1-32*	912/pHL2277	This study
YHL8124	*h⁻ ura4-294 leu1-32*	912/pHL2277	This study
YHL8125	*h⁻ ura4-294 leu1-32*	912/pHL2278	This study
YHL8126	*h⁻ ura4-294 leu1-32*	912/pHL2278	This study
YHL8127	*h⁻ ura4-294 leu1-32*	912/pHL2279	This study
YHL8128	*h⁻ ura4-294 leu1-32*	912/pHL2279	This study
YHL8129	*h⁻ ura4-294 leu1-32*	912/pHL2280	This study
YHL8130	*h⁻ ura4-294 leu1-32*	912/pHL2280	This study
YHL8136	*h⁻ ura4-294 leu1-32 nup124-1*	5750/pHL2435	This study
YHL8102	*h⁻ ura4-294 leu1-32 nup124-1*	5750/pHL2279	This study
YHL8104	*h⁻ ura4-294 leu1-32 nup124-1*	5750/pHL2280	This study

TABLE 2. Primers

Name	Sequence (5′–3′)[a]	Function
HL38	GGAAGAGGAATCCTGGC	Upstream of XhoI in fusion PCR for introducing alanine mutations
HL39	CCAATTGCTTCCAGTCTTTG	Downstream of AvrII in fusion PCR for introducing alanine mutations
HL495	GCTTTAATCAGAGGATCCATGAAAAACTCATCACAGAAAGAATT	Upstream primer for generating Gag in GST vector
HL496	AGTTAGCACAAGGATACCCTCGAGTCAATAACGTCTTTTCTTGTATTTTGTA	Downstream primer for generating Gag in GST vector
HL815	ATTCGAGCTGCCGCAGCGGGTGGATATTGTACTCAA	Top-strand primer for mutant A1
HL816	TCCACCCGCTGCGGCAGCTCGAATTCTTTTCTGTGATG	Bottom-strand primer for mutant A1
HL817	GGAAATGCTGCCGCAGCGACTCAAGATGATATTTCAGA	Top-strand primer for mutant A2
HL818	TTGAGTCGCTGCGGCAGCATTTCCATCCATTCGAATTC	Bottom-strand primer for mutant A2
HL871	TATTGTGCTGCCGCAGCGATTTCAGATATCCTTAAGCA	Top-strand primer for mutant A3
HL872	TGAAATCGCTGCGGCAGCACAATATCCACCATTTCCAT	Bottom-strand primer for mutant A3
HL821	GATGATGCTGCCGCAGCGCTTAAGCATTTTGTAAATCAA	Top-strand primer for mutant A4
HL822	CTTAAGCGCTGCGGCAGCATCATCTTGAGTACAATATC	Bottom-strand primer for mutant A4
HL823	GATATCGCTGCCGCAGCGGTAAATCAAACCACCCGCCAT	Top-strand primer for mutant A5
HL824	TTACCGCTGCGGCAGCGATATCTGAAATATCATCTTGAG	Bottom-strand primer for mutant A5
HL878-1	TCCGCGGATCCGTAAATCAAACCACCCGCCATGTGGAAA	Top-strand primer for Δ30 Gag
HL1061	GTTTAATCCGCGGATCCATGAAAAACTCATCACAGAA	Upstream primer for generating Gag segment 1–50 fusion in GST vector
HL1062	GTTTAATCCGCGGATCCATCGTTAAATTAAGAACATTT	Upstream primer for generating Gag segment 50–100 fusion in GST vector
HL1063	GTTTAATCCGCGGATCCTGGGATGAACTATTAAGAAGAAT	Upstream primer for generating Gag segment 100–150 fusion in GST vector
HL1064	GTTTAATCCGCGGATCCTTATATCTACTATGGATGCTT	Upstream primer for generating Gag segment 150–200 fusion in GST vector
HL1065	GTTTAATCCGCGGATCCTTAAAAACAAAGACTGGAAGC	Upstream primer for generating Gag segment 200–250 fusion in GST vector
HL1066	ACAAGGATCCGCTCGAGTCAGAACTCTTCCATATCCATGC	Downstream primer for generating Gag 1–50 segment fusion in GST vector
HL1067	ACAAGGATCCGCTCGAGTCAATCCCAAGTAAGAGAAGAAT	Downstream primer for generating Gag 50–100 segment fusion in GST vector
HL1068	ACAAGGATCCGCTCGAGTCAAATCTGACTCGTTTCTCACT	Downstream primer for generating Gag 100–150 segment fusion in GST vector
HL1069	ACAAGGATCCGCTCGAGTCAAAAAGATTCCTAGGTTTGGT	Downstream primer for generating Gag 150–200 segment fusion in GST vector
HL1070	ACAAGGATCCGCTCGAGTCACATTTCATAACGTCTTTTCTT	Downstream primer for generating Gag 200–250 segment fusion in GST vector

[a] Underlined sequences indicate sites of mutations.

Plasmids were generated encoding glutathione S-transferase (GST) fused to the N terminus of Gag. PCR products encoding wild-type (WT) and mutant Gags were generated with oligonucleotides that contained a BamHI (HL1105) site at the start and an XhoI site (HL1106) at the predicted end of *gag*. These products were inserted into the BamHI and XhoI sites of pGEX-6P-1 (Pharmacia Biotech) to produce pHL1613-4 (GST-WT), pHL2431 (GST-A1), pHL2432 (GST-A2), pHL2433 (GST-A3), pHL2434 (GST-A4), and pHL2435 (GST-A5). PCR products encoding five 50-amino-acid segments of Gag were generated using pairs of oligonucleotides listed in Table 2. The PCR products were then cloned into the 5′ BamHI and 3′ XhoI sites of pGEX-6P-1, creating pHL2436, pHL2437, pHL2438, pHL2439, and pHL2440. The first amino acid of Gag in pHL2436 was inadvertently changed from methionine (ATG) to threonine (ACG). A PCR product encoding a deletion of the first 30 amino acid residues Gag (Δ30 Gag) was generated using oligonucleotides HL878-1 and HL496. The PCR product was cloned into the 5′ BamHI and 3′ XhoI sites of pGEX-6P-1, creating pHL2552. A PCR product encoding an N-terminal portion of Nup124p was created with a BamHI site at its 5′ end (HL520) and a SalI site at its 3′ end (HL510). This product was inserted into the BamHI and SalI sites of pGEX-6P-1 to produce HL1623-1 (6).

Transposition and recombination assay. Transposition and homologous recombination assays were conducted as described previously (19). All the mutated versions of Tf1 were expressed under the control of the inducible *nmt1* promoter in plasmids with *URA3*. The Tf1 elements contained *neoAI*, a gene that provides resistance to G418 after an artificial intron is spliced out. Patches of cells were grown for 4 days at 32°C on agar plates containing EMM lacking uracil in which the absence of vitamin B1 induced the *nmt1* promoter. For the transposition

TABLE 3. Plasmids

Plasmid	Purpose of plasmid	Reference or source
pFL20	Empty vector	22
pHL449-1	WT Tf1	18
pHL476-3	Integrase frame shift mutant	18
pHL490-80	Protease frame shift mutant	5
pHL1613-4	WT-GST	6
pHL1623-1	N-Nup124	6
pHL1757	NLSless of Gag in pHL449-1	10
pHL2276	Alanine mutant 1 in 449-1	This study
pHL2277	Alanine mutant 2 in 449-1	This study
pHL2278	Alanine mutant 3 in 449-1	This study
pHL2279	Alanine mutant 4 in 449-1	This study
pHL2280	Alanine mutant 5 in 449-1	This study
pHL2431	GST-Gag A1	This study
pHL2432	GST-Gag A2	This study
pHL2433	GST-Gag A3	This study
pHL2434	GST-Gag A4	This study
pHL2435	GST-Gag A5	This study
pHL2436	GST-Gag segment 1–50	This study
pHL2437	GST-Gag segment 50–100	This study
pHL2438	GST-Gag segment 100–150	This study
pHL2439	GST-Gag segment 150–200	This study
pHL2440	GST-Gag segment 200–250	This study
PHL2552	GST-Δ30 Gag	This study

assay, these plates were replica printed to EMM containing 5-FOA to select against the plasmid with Tf1-*neoAI*. After 2 days of growth at 32°C, transposition was measured by a final replica print to plates containing YES, 5-FOA, and G418. These plates were examined after 2 days of growth at 32°C. The assay for homologous recombination was conducted by replica printing patches of cells from the plates with EMM lacking uracil directly to YES medium that contained G418. These plates were examined after 2 days of growth at 32°C.

Indirect immnunofluorescence microscopy. The localization of Gag was visualized by probing cells with polyclonal antibodies raised against Gag in rabbits. Two different Gag antibodies were used to visualize Gag protein. One was an antibody, the production bleed #660, raised against amino acids 20 through 259 (Gag$_{20-259}$) (20), and the other was an affinity-purified antibody raised against a peptide of Gag (amino acids 1 to 15). The affinity-purified antibody against peptide 1 to 15 was prepared from the production bleeds #12 and #13 of rabbit 63085 (BioSource International). The monoclonal antibody for Nop1p, D77, was kindly provided by J. P. Aris (3). Alexa Fluor TM 594 goat anti-rabbit immunoglobulin G IgG (H+L) conjugate and Alexa Fluor 488 goat anti-mouse IgG (H+L) (Molecular Probes) were used as secondary antibodies for fluorescence. Nuclear DNA was visualized with Vectashield mounting medium containing 1.5 μg/ml DAPI (4′,6′-diamino-2-phenylindole) from Vector Laboratories (H-1200). Cells transformed with an empty plasmid, pHL1032, were used as a negative control for background fluorescence. Cells totaling approximately 1.5 optical density units (optical density [OD] at 600 nm) were harvested and fixed in 3.7% formaldehyde (Sigma F1268) at 32°C for 45 min on a roller. The cells were then washed twice in K-buffer (0.1 M potassium phosphate, pH 6.5). The cell walls were removed by incubation in K-sorbitol buffer with Zymolase (0.1 M potassium phosphate, 1.2 M sorbitol, 0.01% βeta-mercaptoethanol, and 3 mg/ml of 100T Zymolase) at 32°C for 40 min on a roller. Once the cell wall was removed, the spheroplasts were washed seven times in K-sorbitol buffer (0.1 M phosphate buffer and 1.2 M sorbitol) and then resuspended in 200 μl of the buffer before the spheroplasts were transferred onto polylysine-coated slides (ICN 6040805). The spheroplasts were then incubated in PBST buffer (0.1 M potassium phosphate, 0.15 M NaCl, 0.1% Tween 20, and 10 mg/ml bovine serum albumin; Sigma A3059) overnight at 4°C. The cells were then immunostained using primary antibody (Gag antibody, 1:200; purified peptide antibody, 1:500; and Nop1 antibody, 1:500) for 4 h at room temperature (27°C). After incubation with the primary antibodies, the slides were washed six times with PBST and then probed with secondary antibodies (1:500) for 1 h before they were washed seven times with PBST. Cells were then mounted on glass slides with Vectashield mounting medium with DAPI, and the slides were sealed. The cells were examined with a Zeiss Axioscope equipped with UV and fluorescence isothiocyanate optics. Images were collected by QED (QED Imaging) and Open Lab software (Improvision).

Assay for binding of Gag to Nup124p. Binding experiments with GST fusions were carried out as described previously (6). Wild-type Gag and the Gag with the alanine mutations were expressed in the BLR(DE3) strain of *E. coli* as fusions to the C terminus of GST. Cultures (each, 500 ml) were inoculated from permanent freezer stocks and allowed to grow overnight with shaking at 25°C. When cultures reached an OD$_{600}$ of 0.3 to 0.6, protein production was induced by adding IPTG (isopropyl-ā-D-thiogalactopyranoside) to a final concentration of 0.1 mM. Cells were harvested after 4 h or after overnight induction, and the GST fusion proteins were purified with 2 ml of a 50% slurry of glutathione-Sepharose 4B beads.

The GST-Nup124p protein was first purified and then cleaved off the resin with PreScission protease (Pharmacia Biotech) to remove the GST domain. The GST-Gag proteins were purified on the glutathione-Sepharose 4B beads and used directly in the binding assay.

The binding of the N-terminal half of Nup124 to GST-Gags was performed in a binding buffer that contained 20 mM HEPES (pH 6.8), 150 mM potassium acetate, 2 mM magnesium acetate, 2 mM dithiothreitol, 0.1 mM Tween 20, and 0.1% Casamino Acids. The beads with GST-Gag were washed in binding buffer, and the N-Nup124p protein was dialyzed in binding buffer. After the dialysis, 15 μl of dialyzed Nup124p was added to an equal volume of resin with GST-Gag. The amount of N-Nup124p in each binding reaction was approximately 1 μg, and the amount of the GST-Gag fusions was approximately 2 μg. The samples were incubated for 40 min at room temperature with gentle mixing. When the incubation of the samples was completed, the beads were washed three times with 250 μl of binding buffer. The pellets were then analyzed by gel electrophoresis.

DNA blotting. The cDNA produced by the Tf1 elements with the alanine mutations was measured on DNA blots as described previously (5). Total DNA was extracted from cells grown to stationary phase in the absence of vitamin B1. The total DNA extracted was digested with BstXI, and the products were separated on 0.8% agarose gels. The DNA fragments were transferred to Gene-

screen plus (NEN Life Science products) overnight by capillary transfer and then probed with the 1-kb BamHI fragment of *neo* (5). The DNA blot was carried out using the Dig High Prime labeling and detection kit (Roche).

Whole-cell extracts. Extracts of whole cells were prepared from cells harvested at different growth stages. The cells harvested from 50-ml cultures were resuspended in breaking buffer containing 15 mM NaCl, 10 mM HEPES-KOH (pH 7.8), and 5 mM EDTA. The cultures were resuspended in a volume of 4 μl per OD$_{600}$ unit. Half of the resuspended cells were placed in a 2-ml tube (Starstedt no. 72.694.006) containing acid-washed glass beads (425 to 600 μm; Sigma G-8772) and broken with a mini-BeadBeater (Biospec Products). The Bead-Beater was set at the highest setting, and cycles, each cycle consisting of 30 s on and 30 s, off were repeated three times for the cells harvested at the log phase and four times for the cells harvested at the stationary phase. The cell extracts were separated from the mixture of the broken cell debris and glass beads by centrifugation at 1,000 × g for 5 min. Cell extracts were recovered from the top layer of the tube. This pellet was resuspended in the breaking buffer used for breaking cells, and the mixture of the broken cell debris and glass beads was separated from the cell extract again by repeating the centrifugation. This supernatant was recovered and added to the cell extract in the supernatant of the first 1,000 × g centrifugation. The total amount of protein in the cell extracts was determined by the Bradford assay (Bio-Rad).

Differential sedimentation and immunoblot analysis. Cell extracts as described above were subjected to centrifugation at 12,000 × g for 10 min. The supernatant was removed for differential sedimentation and immunoblot analyses. Breaking buffer was added back to the pellet to the exact volume of supernatant removed. Equal volumes of 2× sample loading buffer were then added to the supernatant and the pellet samples. The protein samples with sample buffer were boiled for 3 min, and 12.5 μg of total protein from the supernatant was loaded on a 10% sodium dodecyl sulfate (SDS)-polyacrylamide gel for SDS-polyacrylamide gel electrophoresis (PAGE) analysis. The proportion of the pellet fraction loaded was equal to the proportion of the supernatant on the gel. The proteins in the gels were then transferred to Immobilon-P membranes (Millipore). The membrane was probed with Gag antibody (1:5,000) and the affinity-purified peptide antibody (1:10,000). A description of the antibodies is included in the section on immnunofluorescence. The secondary antibody was horseradish peroxidase-conjugated donkey anti-rabbit Ig (1:10,000). ECL was used to detect the protein signals (Amersham).

Gradient sedimentation. The OptiPrep application M4, the method used for the purification of recombinant adeno-associated virus in preformed iodixanol gradients (OptiPrep; Axis-Shield, Oslo, Norway), was used as the gradient medium to isolate Tf1 particles (Axis-Shield, Oslo, Norway) (39) with the OptiPrep M4 purification application. Briefly, step gradients were prepared from a 60% (wt/vol) sterile solution of iodixanol (OptiPrep; Axis-Shield, Oslo, Norway). Whole-cell extracts were prepared as described above, and 0.5 ml of the extracts was transferred into Ultra-Clear centrifuge tubes (7/16 by 1 3/8 in; Beckman 347356) and layered on top of step gradients of 54% (0.28 ml), 40% (0.28 ml), 25% (0.4 ml), and 15% (0.5 ml) iodixanol in 1× PBS-MK buffer (1× phosphate-buffered saline, 1 mM MgCl$_2$, 5 mM KCl). The 15% OptiPrep also contained 1 M NaCl. The tubes with the samples were placed in a TLS55 rotor and centrifuged at 125,000 × g for 1 h. Nine 200-μl fractions were obtained by removing samples from the top with a Pipetman.

Electron microscopy. Cells expressing wild-type Tf1 were harvested after 24 (log phase; OD$_{600}$, 1.07) and 48 (stationary phase) hours of growth in EMM. The electron microscopy (EM) sections of cells expressing different alanine mutants were harvested after 48 h of growth in EMM. Twelve OD units of cells were washed once in 10 ml of PEM {0.1 M PIPES [piperazine-*N*,*N*′-bis(2-ethanesulfonic acid)], pH 6.9, 2 mM EGTA, 1 mM MgCl$_2$}, and fixed in 2% glutaraldehyde (Tousimis, Rockville, MD) in PEM for 2 h at room temperature. Cells were then washed and resuspended in 5 ml of PEM containing 0.2% tannic acid (Electron Microscopy Sciences, catalog no. 21710) and incubated 15 min at room temperature. Following two washes in 5 ml of 0.1 M KPi, pH 7.5, cell walls were then digested in 2 ml KPi, 0.25 mg/ml zymolase 100T (U.S. Biological no. Z1004), 90 mM β-mercaptoethanol for 60 min at 30°C. Cells were then washed in 0.1 M cacodylate, pH 6.8, and resuspended in 1 ml of 2% osmium peroxide (Electron Microscopy Sciences, Ft. Washington, PA) in 0.1 M cacodylate for 1 h at room temperature. Cells were then washed in water and resuspended in 1 ml of 2% uranyl acetate for 1 h at room temperature, washed in water, and dehydrated progressively in a series of increasing concentrations of ethanol solution (35%, 50%, 70%, 90%, and 95% and 3 times in 100%) and then in propylene oxide (100%). The cells were infiltrated in an equal volume of 100% propylene oxide and epoxy resin (Electron Microscopy Sciences, Ft. Washington, PA) overnight and embedded in pure resin on the following day. The epoxy resin was cured in a 60°C oven for 48 h. The cured block was thin sectioned and stained in

uranyl acetate and lead citrate. The sections were examined and imaged with a transmission EM (H7000; Hitachi, Tokyo, Japan), equipped with a charge-coupled device camera (Gatan, Pleasanton, CA).

RESULTS

Alanine substitutions adjacent to the NLS of Gag resulted in defective transposition. The Gag of Tf1 possesses an N-terminal NLS that is required for nuclear localization (10). Nup124p is a nuclear pore protein that is required for the localization of Gag in the nucleus (6). Experiments with fusion proteins revealed that the residues of Gag following the NLS caused nuclear localization to require Nup124p. To examine the role of the amino acids following the NLS, alanine mutations were created in Gag from amino acids 11 to 30. Five mutant versions of Tf1 were generated, and each had a tract of four sequential amino acids replaced by four alanines. The mutations were named A1, A2, A3, A4, and A5, as illustrated in Fig. 1.

To test whether the NLS-associated residues were important for import function, all five versions of Tf1 were assayed for transposition (Fig. 2). The levels of transposition were measured with an assay that is based on expression of Tf1 from an inducible promoter in a high-copy-number plasmid (18). The copy of Tf1 in the plasmid contained a *neoAI* gene so that after Tf1 was expressed and 5-FOA was used to select against cells containing the expression plasmid, cells with insertions of Tf1-*neoAI* in the genome could be identified by their resistance to G418. The bulk of the cells that became resistant to G418 were the result of true integration. This was indicated by the significant reduction in G418 resistance due to a frameshift mutation that blocked the expression of IN Tf1-INfs (Fig. 2) (4). A frameshift in PR inhibited expression of RT and indicated that reverse transcription is required for cells to become resistant to G418. The transposition activities of the Tf1 elements containing the five alanine mutations were significantly less than those of the wild-type Tf1-*neoAI* (Fig. 2A). This indicated that the region of Gag from residues 11 to 30 was critical for transposition.

We asked whether the alanine mutations inhibited early steps in the transposition cycle by using a modified version of the transposition assay that measures the amount of cDNA present in the nucleus. This assay measures homologous recombination between Tf1 cDNA and the Tf1 plasmid. In the homologous recombination assay, the plasmid expressing Tf1-*neoAI* is not removed before cells are replica printed to medium containing G418. Since Tf1-*neoAI* in the expression plasmid has an artificial intron that disrupts *neo*, the cells are initially sensitive to G418. They become resistant only after the intron is spliced, the mRNA is reverse transcribed, and the cDNA recombines homologously with the expression plasmid (4). The resistance to G418 did not depend on IN expression, as indicated by the G418 resistance produced by Tf1-INfs (Fig. 2B). The level of recombination with the Tf1 cDNA was significantly reduced for all of the alanine mutants (Fig. 2B), although A2 exhibited some residual activity. These results suggested that the alanine mutations inhibited either reverse transcription or the import of the cDNA into the nucleus.

The expression of Gag is not altered by the alanine mutations. To determine whether the mutations reduced transpo-
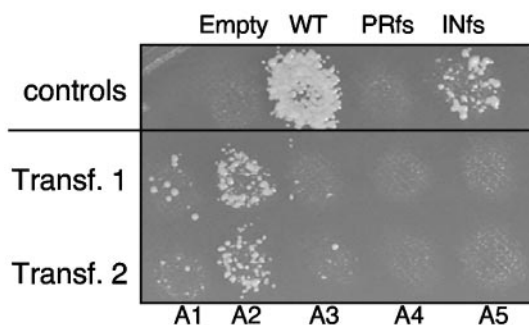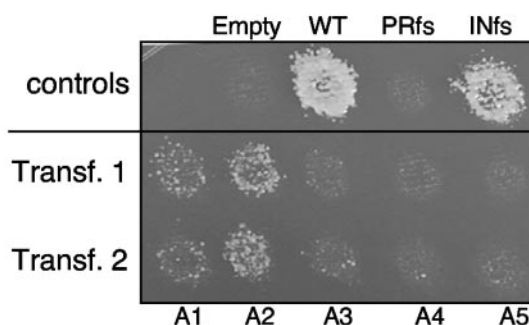

FIG. 2. The transposition and homologous recombination activity of the alanine mutants. Two independently transformed strains (Transf. 1 and 2) with the mutated transposons, A1 (YHL8121 and YHL8122), A2 (YHL8123 and YHL8124), A3 (YHL8125 and YHL8126), A4 (YHL8127 and YHL8128), and A5 (YHL8129 and YHL8130), were tested for transposition and homologous recombination activity. The control strains included empty vector (YHL1032), wild-type Tf1 (YHL1282), Tf1 with a frameshift in protease (YHL1836), and Tf1 with a frameshift in integrase (YHL1554). (A) Transposition activity of Tf1 marked with *neoAI* was measured by inducing the expression of the element from the *nmt1* promoter in the plasmid pHL449-1. After induction, the expression plasmid was removed with 5-FOA, and the frequency of transposition was measured on EMM supplemented with G418, as shown in panel A. (B) The accumulation of cDNA and its presence in the nucleus was detected by a homologous recombination assay. Once expression of Tf1-*neoAI* was induced from pHL449-1, patches of cells were replica printed to medium containing G418. Recombination between cDNA and pHL449-1 allowed growth on this medium.

sition by lowering the expression of Gag, all five alanine mutants were examined by immunoblot analysis. The expression of Gag was examined in cells harvested at log phase (OD$_{600}$, 1.0). Figure 3A shows the levels of Gag detected with antibodies raised against amino acids 20 to 259. All of the alanine mutants accumulated amounts of Gag similar to that of WT, indicating that there was no defect in Gag expression (Fig. 3A, top). The experiment was repeated with cultures grown to stationary phase to measure Gag levels under the conditions where transposition is thought to occur. At the stationary phase of cell growth, Tf1-*neoAI* with the A4 and A5 mutations showed sensitivity to proteases (Fig. 3A, bottom). Although the level of Gag-A5 was the same as wild type, its molecular mass was reduced to approximately 20 kDa. This degradation
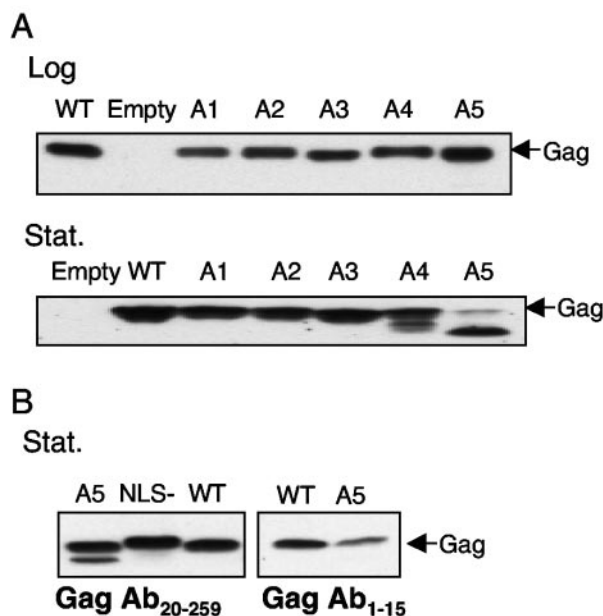
FIG. 3. The immunoblot of Gags expressed by the mutant transposons. (A) The levels of Gag in cells were measured by immunoblot analysis of whole-cell extracts. Both log-phase (OD_{600}, 1.0) and stationary-phase (OD_{600}, 10) cells were extracted from cultures containing WT (YHL1282), empty plasmid (YHL1032), A1 (YHL8121), A2 (YHL8123), A3 (YHL8125), A4 (YHL8127), and A5 (YHL8129). After electrophoresis on a 10% SDS-PAGE gel, the extracts were transferred to membranes and probed with an antibody specific for Gag residues 20 to 259 (Gag Ab_{20-259}). (B) The levels of Gag produced in stationary-phase cells by wild-type Tf1 and A5 were analyzed with immunoblotting. The membranes were probed with Gag Ab_{20-259} and an antibody specific for the first 15 amino acids of Gag (Gag Ab_{1-15}). NLSless (NLS−) was a version of Tf1 with a mutation in the NLS (10). This strain was included as a control to show that Gag can accumulate in the cytoplasm without degradation.
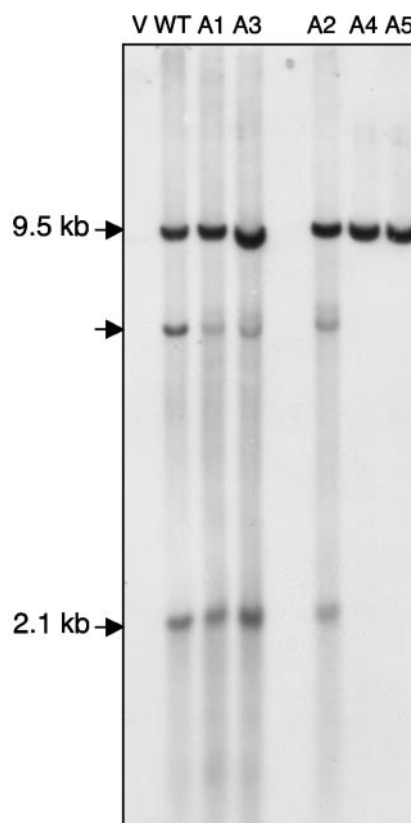

FIG. 4. A blot of the cDNA produced by the five different alanine mutants. Total DNA was extracted from cells containing empty plasmid (V; YHL1032), WT (YHL1282), A1 (YHL8121), A2 (YHL8123), A3 (YHL8125), A4 (YHL8127), and A5 (YHL8129). Total DNA was digested with BstXI, subjected to electrophoresis on agaose, and probed with the *neo* gene. The 9.5-kb band was produced by the plasmid, and the 2.1-kb band was a fragment of the Tf1 cDNA. The band labeled with just an arrow was thought to be single LTR circles.

was specific for cells in stationary phase. The 20-kDa species of Gag-A5 was not detected by an antibody raised against the first 15 amino acids of Gag (Fig. 3B, right, lane A5). This suggests that the A5 mutation resulted in proteolysis of Gag that removed the N terminus of the protein.

Alanine mutations A4 and A5 significantly reduced levels of cDNA. The alanine mutations significantly reduced homologous recombination between the cDNA and the expression plasmid (Fig. 2B). One possibility was that the mutations in Gag resulted in reduced reverse transcription. To test this directly, the level of cDNA produced by Tf1-*neoAI* with the alanine mutations was measured on DNA blots of total DNA (Fig. 4). To distinguish the plasmid from the cDNA forms of Tf1, the DNA was digested with BstXI. The DNA blot was then hybridized with a fragment of *neo* as a probe. The cDNA fragment of Tf1 detected by this probe was 2.1 kb, and the plasmid DNA was visualized as a 9.5-kb band. The plasmid band was used as an internal control for the level of total DNA loaded in individual lanes. The results demonstrated that the cells expressing A1, A2, and A3 produced wild-type levels of cDNA. However, no detectable cDNA was observed from the cells expressing A4 and A5. The lack of cDNA was at least one

reason why the elements with mutations A4 and A5 were unable to transpose.

The alanine mutations alter the nuclear localization of Gag. The study of Gag fused to LacZ suggested that amino acids 11 to 30 modulated nuclear localization (10). We examined the role of these amino acids in the nuclear localization of Gag by using the transposons with the alanine mutations. As expressed by the transposon, Gag is localized in the nucleus when the cells grow to stationary phase (6, 9). The Gag in cells grown to stationary phase was examined with indirect immunofluorescence and found to associate closely with the DNA signal as observed with DAPI (Fig. 5A). In these cells, Gag was located in a small compartment in or immediately adjacent to the DAPI signal. We tested whether this localization correlated with the nucleolus by using an antibody specific for Nop1p, a fibrillarin that is positioned specifically in the nucleolus (3). As shown in Fig. 5A, Gag localization correlated well with the position of Nop1p. The association of Gag with Nop1p not only indicates that Gag is located in the nucleus but also shows that the localization is near or in the nucleolus. To measure what proportion of cells exhibited nuclear localization, we examined approximately 100 cells for strong signals of Gag that
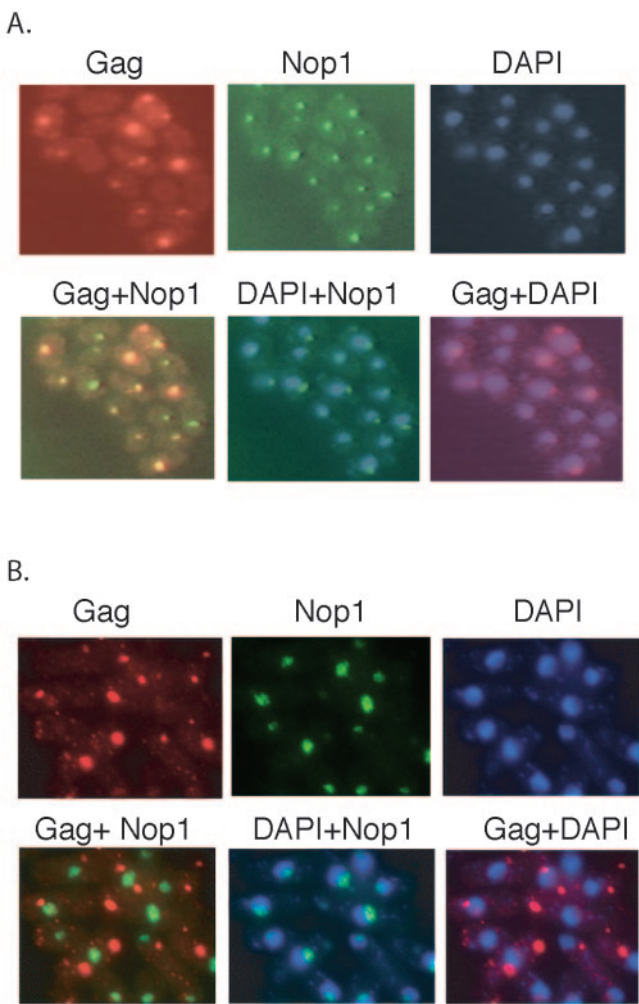
A.

B.

FIG. 5. Indirect immunofluorescence of wild-type Gag in cells harvested at stationary phase and log phase. The immunolabeling of Gag was produced by a polyclonal antibody against Gag Ab$_{20–259}$ (red). DNA in the cells was stained with DAPI (blue). Nop1 was detected by immunolabeling with a monoclonal antibody (green). Overlay images were created for Gag+Nop1, DAPI+Nop1, and Gag+DAPI. (A) The Gag, Nop1, and DNA of wild-type Tf1 (YHL1282) were visualized in stationary-phase cells. (B) The Gag, Nop1, and DNA of wild-type Tf1 were visualized in log-phase cells.

TABLE 4. Percentage of cells with nuclear localization of Gag

Version of Gag	% Nuclear localization	
	Log phase	Stationary phase
WT	16.9	96.5
A1	14.0	19.2
A2	14.0	20.0
A3	6.0	14.8
A4	73.3	87.6
A5	89.2	97.6
Empty plasmid	<1.0	<1.0

tors. The Gags of A4 and A5 retained their ability to localize in the nucleus. Since little is known about the signals in stationary phase that trigger the localization of Gag in the nucleus, we also tested whether the alanine mutations changed the localization of Gag in cells from cultures harvested at log phase. As expected, the wild-type Gag, Gag-A1, Gag-A2, and Gag-A3 proteins localized primarily in the cytoplasm (Table 4). But what was particularly surprising was that even in log-phase cells, Gag-A4 and Gag-A5 were associated with the nucleus (Fig. 7; Table 4). The positions of Gag-A4 and Gag-A5 in the nucleus were concentrated in the nucleolus, as indicated by the colocalization of Gag and Nop1. These results indicate that the A4 and A5 mutations suppressed the requirement of stationary phase for nuclear localization.

An unusual property of Gag-A4 in cells from log-phase cultures is that 30% of the cells contained Gag associated with fibrous structures (Fig. 7). Although the fibrous structures were much more frequent in cells from log-phase cultures, 2% of cells in stationary phase with signals of Gag-A4 also possessed these fibers (data not shown).

Amino acids 200 to 250 of Gag interact directly with the N-terminal half of Nup124p. The nuclear pore factor Nup124p is required for the nuclear localization of Gag and as a recombinant protein; the N-terminal half of Nup124p interacts directly with Gag (6). To determine whether the alanine mutations disrupted the nuclear localization of Gag by reducing the interaction between Gag and Nup124p, we tested the Gag proteins with the alanine mutations for binding to Nup124p. The Gag proteins were purified from *Escherichia coli* as GST-Gag fusions and tested for binding to the N-terminal fragment of Nup124p, which was also purified as a recombinant protein. The SDS gels shown in Fig. 8A contained the GST-bound Gag proteins and show that each of the mutated versions bound approximately the same amount of Nup124p as did the wild-type Gag.

An additional experiment was conducted to test whether the region of Gag that interacts with Nup124p is located inside the first 30 amino acids of Gag. In the same type of precipitation assay used above, GST-Gag with a deletion of the first 30 amino acids (Δ30) was found to bind to the N-terminal half of Nup124p, as well as wild-type Gag (Fig. 8B). These results indicate that the binding of Nup124p by Gag occurs outside of the first 30 amino acids. To determine which regions of Gag interact with Nup124p, Gag was divided into five 50-amino-acid segments, and each was fused to GST. When these segments were tested for binding to the N-terminal half of

overlapped or associated with the DAPI signal (Table 4). We found 96.5% of the cells had a substantial signal of Gag associated with the nucleus. Cells harvested in log phase showed significantly less association with Nop1p and the DAPI stain (Fig. 5B; Table 4).

Having established the localization of wild-type Gag, we asked whether the alanine mutations caused any changes. When we examined the Gag of cells in stationary-phase cultures, alanine mutants A1, A2, and A3 exhibited significant defects in nuclear localization (Fig. 6; Table 4). The cytoplasmic localization of Gag lacking the N-terminal NLS (NLSless) was uniform in nature and in strong contrast to the punctate appearance of Gag in mutants A1, A2, and A3. Since the NLSless version of Tf1 has been shown to form particles that produce cDNA and sediment with normal behavior (10), it is possible that the punctate appearance is due to transport fac-
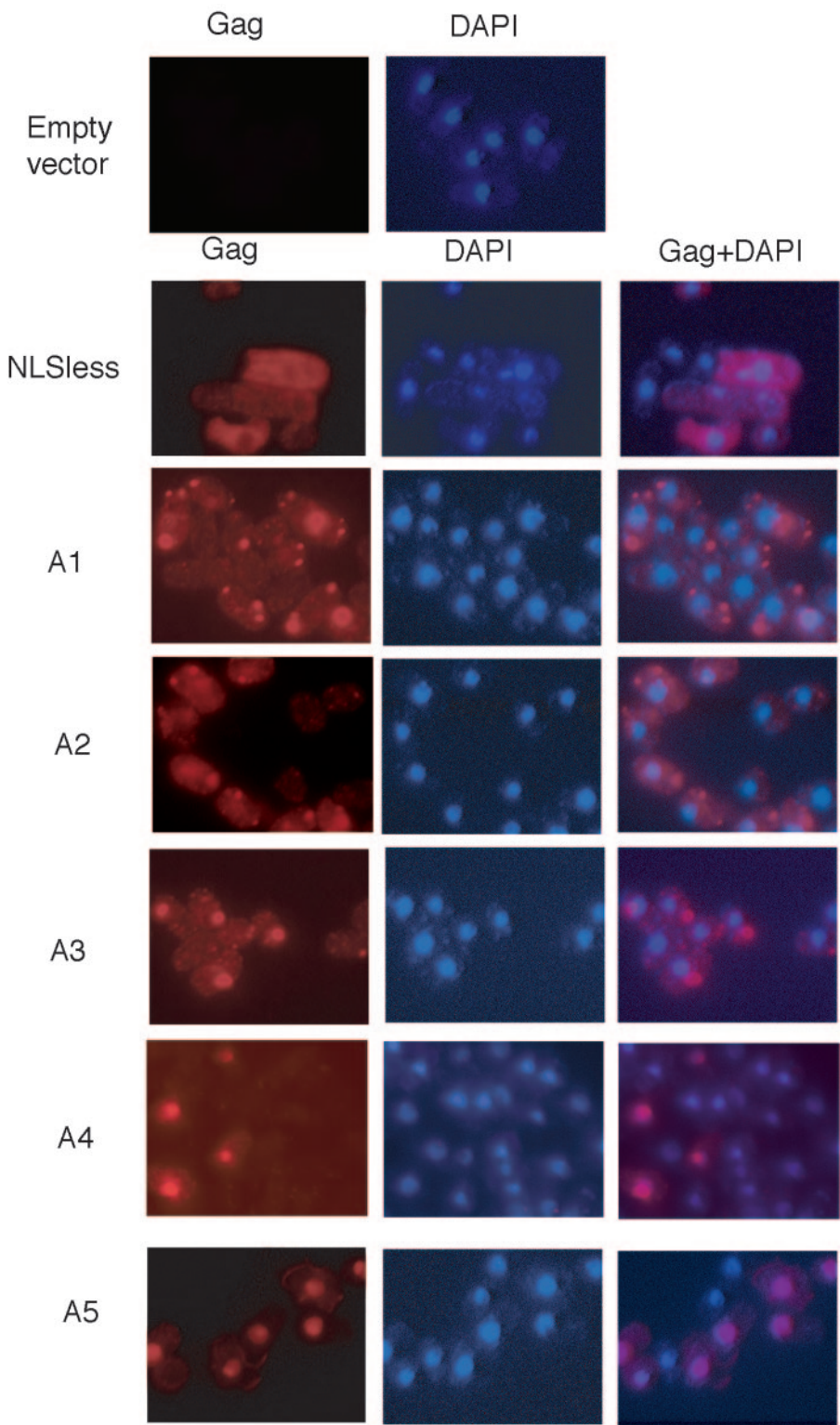
FIG. 6. Indirect immunofluorescence of Gag in cells expressing the alanine mutants. The cellular localizations of Gag, Nop1, and DNA were determined in stationary-phase cells expressing A1 (YHL8121), A2 (YHL8123), A3 (YHL8125), A4 (YHL8127), and A5 (YHL8129). The immunolabeling of Gag was as described for Fig. 5.
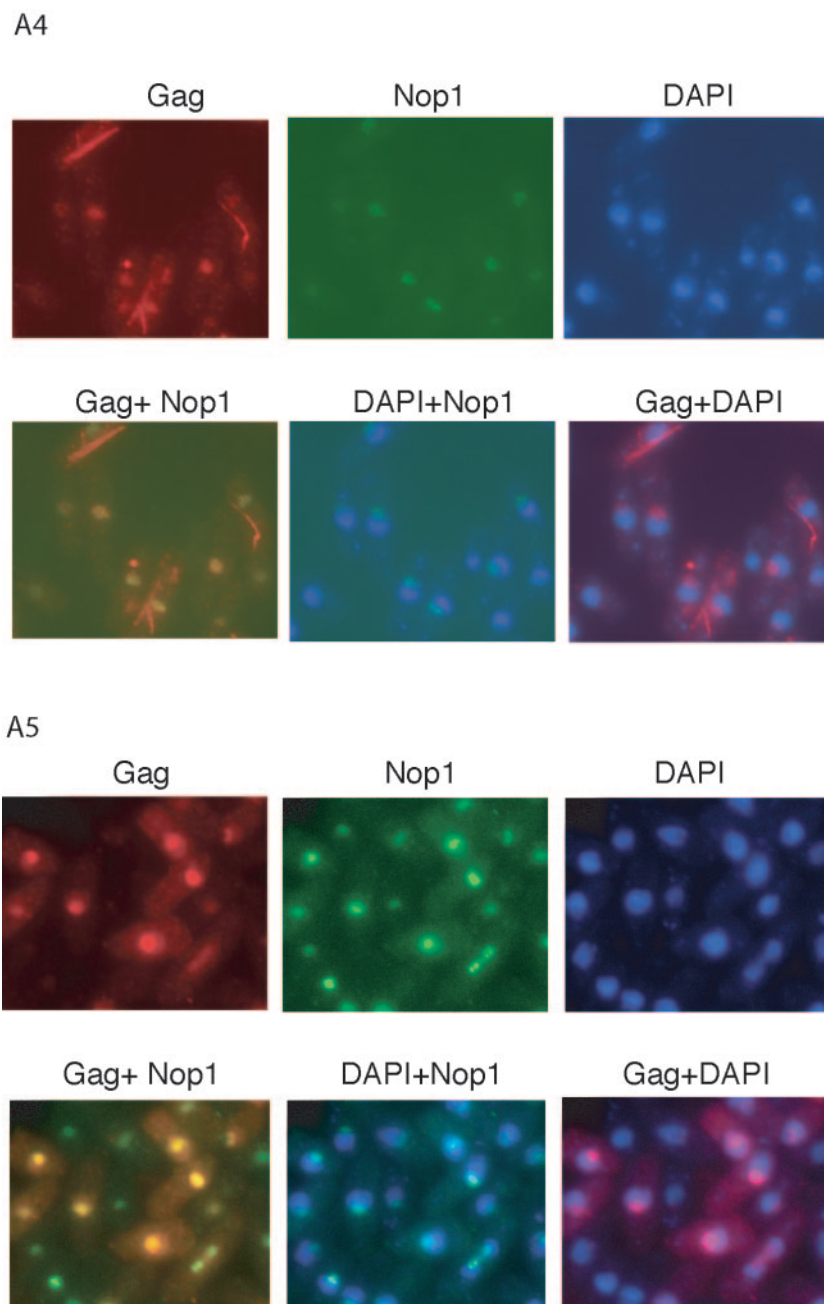
FIG. 7. Indirect immunofluorescence of Gag in log-phase cells expressing the alanine mutants A4 and A5. The localization of Gag, Nop1, and DNA was determined in cells expressing either A4 or A5. The immunolabeling of Gag was as described for Fig. 5.

Nup124p, the segment spanning amino acids 200 to 250 of Gag was the only GST fusion that showed significant binding (Fig. 8C). These data indicate that the amino acids of Gag that were replaced by alanines did not contribute to the binding to Nup124p.

The alanine mutations caused defects in the formation and aggregation of VLPs. The reduced localization of Gag in the nuclei of cells expressing A1, A2, and A3, and the premature localization of Gag in the nuclei of cells expressing A4 and A5 could be due to changes in the structure of the virus-like particles (VLPs). The assembly of Gag, RT, IN, and cDNA

into VLPs is detected as large macromolecular complexes (20). We tested whether the alanine mutations altered the formation of the macromolecular complex by subjecting cell extracts to differential centrifugation. We prepared whole-cell extracts from strains expressing the different versions of Tf1 and subjected them to centrifugation at $12,000 \times g$ for 10 min. These extracts were generated from cultures of late-log-phase cells (OD_{600}, 8.0) to avoid the cleavage of Gag-A5 that occurs in stationary-phase cells. Equal proportions of the total extract, the pellet, and the supernatant were examined on an immunoblot probed with the antibody specific for Gag_{20-259}. The
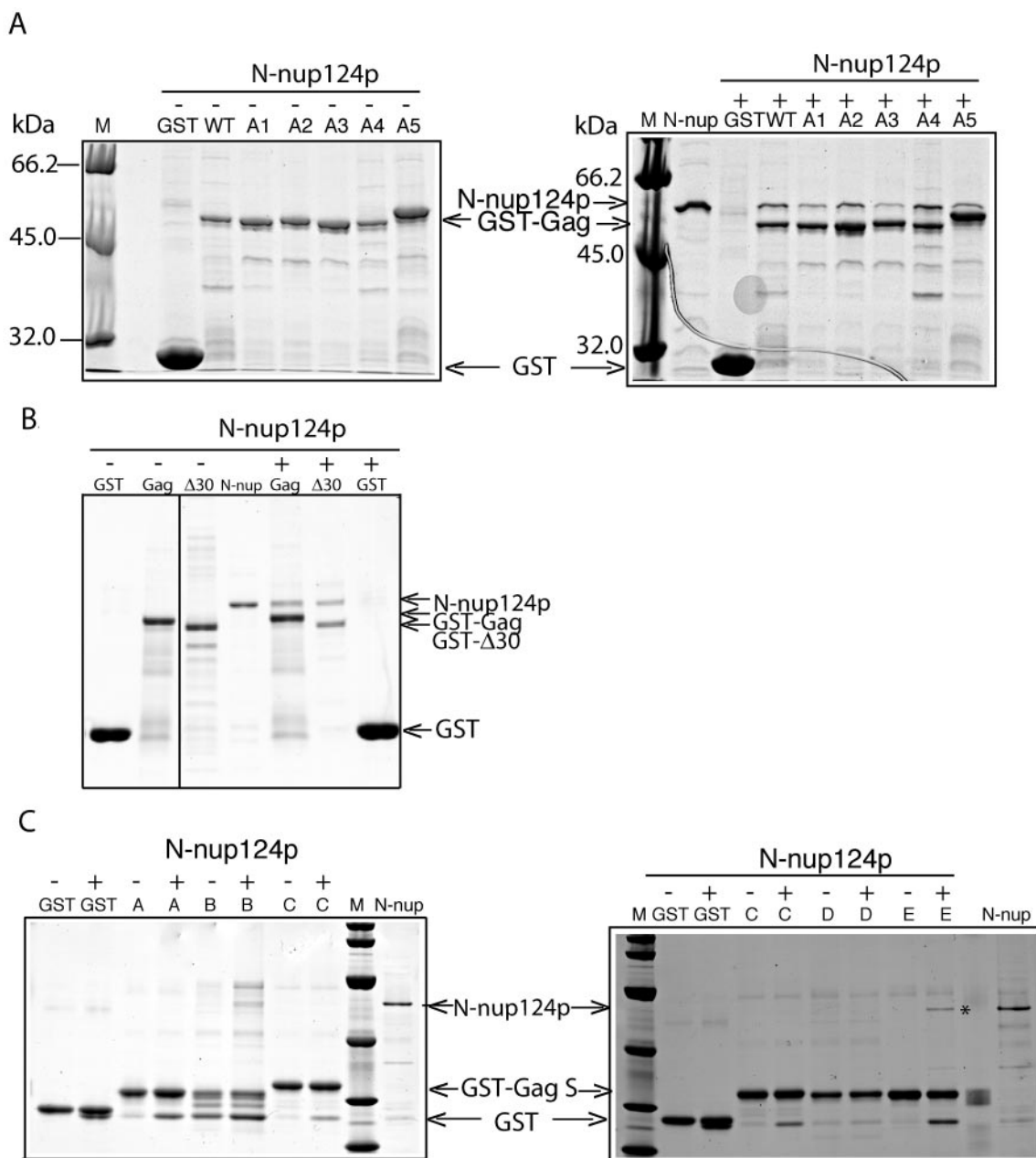
FIG. 8. Binding assays for interactions between Nup124p and Gag. The N-terminal half of Nup124p (N-nup124p) and versions of Gag proteins were fused to the C terminus of GST, expressed in bacteria, and purified. N-Nup124p with GST removed was incubated with each of the GST-Gags of the alanine mutants. The GST-Gags were precipitated with glutathione-Sepharose 4B beads, and the N-Nup124p associated with the Gag was visualized on SDS-PAGE gels stained with Coomassie blue. M, broad-range molecular-mass markers (Bio-Rad); N-nup, purified N-Nup124p. The plus and minus signs indicate the presence or absence of N-Nup124p in the binding reaction. (A) Each of the Gags with the alanine mutants was tested for binding with N-nup124p. The gel was a 10% SDS–polyacrylamide gel. (B) GST-Gag without the first 30 amino acids of Gag (Δ30) was tested for binding to N-Nup124p. This gel was a 10 to 20% gradient SDS-PAGE gel. (C) Five 50-amino-acid segments of Gag were tested for binding to N-Nup124p. The segments of Gag tested were A (amino acids 1 to 50), B (amino acids 50 to 100), C (amino acids 100 to 150), D (amino acids 150 to 200), and E (amino acids 200 to 250). These gels were NuPAGE 4 to 12% bis-Tris gels. The asterisk marks the N-Nup124p that bound to the segment containing amino acids 200 to 250.

majority of the wild-type Gag was found in the pellet fraction (Fig. 9A). This was also true for Gag-A1, Gag-A2, and Gag-A3. These results suggest that the mutations A1, A2, and A3 did not cause extensive changes to the properties of the VLPs. On the other hand, the majority of Gag-A4 and Gag-A5 was

present in the supernatant fraction (Fig. 9A). This indicates that the mutations A4 and A5 did cause a significant reduction in the formation of the VLP complexes.

The technique of differential sedimentation cannot distinguish between defects in the formation of individual VLPs
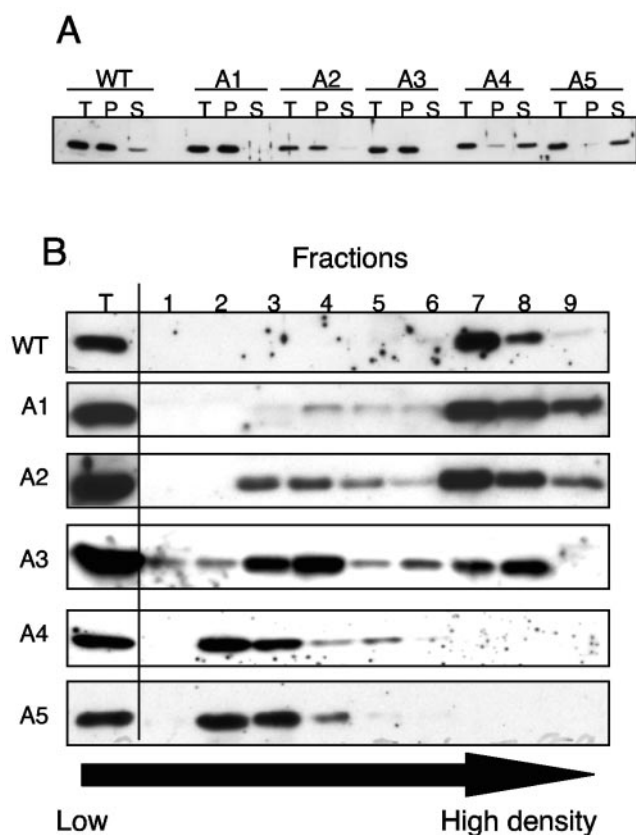
A

B

FIG. 9. Differential sedimentation and gradient fractionation experiments of Gags with the alanine mutations. (A) Whole-cell extracts prepared from WT (YHL1282), A1 (YHL8121), A2 (YHL8123), A3 (YHL8125), A4 (YHL8127), and A5 (YHL8129) were centrifuged at $1,000 \times g$ for 5 min. The supernatants were further centrifuged at $12,000 \times g$ for 10 min. The samples loaded on an SDS-PAGE gel were the total cell extracts (T), the pellets from the $12,000 \times g$ centrifugation (P), and the supernatant from the $12,000 \times g$ centrifugation (S). (B) The supernatants from the $1,000 \times g$ centrifugation described above were also sedimented on gradients of iodixanol centrifuged at $125,000 \times g$. The 0.2-ml fractions were collected from low density (fraction 1) to high density (fraction 9). The fractions were immunoblotted and probed with the Gag Ab$_{20-259}$ antibody. Total cell extracts (T) from cells expressing the mutant transposons were centrifuged at $125,000 \times g$ in OptiPrep gradients to isolate virus-like particles.

versus aggregates of VLPs. To assess whether the alanine mutations affected the formation of individual VLPs we used gradient sedimentation. Cells were harvested at the late-log-phase of cell growth (OD$_{600}$, 6.0 to 8.0), and their extracts were sedimented through gradients of iodixanol. The majority of wild-type Gag was found in fractions seven and eight (Fig. 9B). The behaviors of Gag-A1 and Gag-A2 were similar to that of wild-type Gag. Gag-A3 existed in two populations and sedimented to fractions three and four, as well as to fractions seven and eight. This behavior indicates that the A3 mutation partially disrupted the structure of the VLPs. The sedimentation of Gag-A4 and Gag-A5 was significantly reduced compared to that of wild-type Gag (Fig. 9B). For both A4 and A5, the entire population of Gag sedimented to fractions two and three. These results indicated that the Gags of A4 and A5 did not assemble into VLPs.

The sedimentation analysis described above can measure whether the alanine mutations caused significant changes in the size of the macromolecular complex but may not detect changes in the structure of the VLPs. The VLPs of Tf1 can be readily observed by transmission EM as clusters of highly organized spherical structures (34). We used EM to ask whether the alanine mutations caused morphological changes in the VLPs. Cells expressing wild-type Tf1 were harvested from stationary-phase cultures, and sections were examined for VLPs by EM (Fig. 10). The VLPs formed clusters of distinctive and defined particles approximately 50 nm in diameter. We found that these particles existed in 1.4% of 3,800 sections of cells that we examined. A total of 1,360 cells that did not express Tf1 were examined, and none contained VLPs. We also observed that of the stationary-phase cells with VLPs, approximately 79% had tubular structures surrounding the clusters of VLPs (Fig. 10). These structures have been reported previously, but their function and composition remain unknown (34).

VLPs produced by cells in stationary phase expressing mutants A1, A2, and A3 were observed and compared to those of wild-type Tf1. Although present, the particles of the mutants were not as defined and did not appear well ordered (Fig. 10). The VLPs from these mutants tended to be smaller and more electron dense than the particles produced by wild-type Tf1. The proportion of approximately 1,000 sections of cells that contained VLPs of A1, A2, and A3 was 6.8%, 5.4%, and 4.1%, respectively. Despite the careful examination of sections of cells expressing A5, no particle structures were observed. The absence of VLPs was consistent with the lack of macromolecular complexes as observed by gradient fractionation and differential centrifugation (Fig. 9).

The gradient fractionation of cells expressing A4 was similar to that of A5 in that no large species of macromolecular complexes were observed. As a result, we were surprised to find that A4 did produce VLPs and that they were spherical and well ordered (Fig. 10 and 11). Of the 1,187 sections of cells examined, 2.3% possessed these particles. However, the number of particles in each cluster of VLPs was significantly smaller than what was produced by wild-type Tf1. In addition to the smaller clusters, the total number of VLPs per cell section was smaller in cells expressing A4. An average of 14 VLPs per cell were observed in 1,187 cell sections expressing A4, while an average of 73 VLPs per cell section were observed in 3,861 cell sections expressing wild-type Tf1.

The mutations A4 and A5 caused nuclear localization of Gag to become independent of Nup124p. The nuclear localization of Gag is inhibited until cultures reach stationary phase. It was therefore surprising that mutations A4 and A5 allowed nuclear localization in cells from log-phase cultures. One explanation for this nuclear localization during log phase is that the A4 and A5 mutations allowed Gag to enter the nucleus by an alternative pathway. We tested this possibility by asking whether Gag-A4 and Gag-A5 entered the nucleus by the same Nup124p-dependent pathway that is used by wild-type Gag. The localizations of Gag-A4 and Gag-A5 were tested in a strain of *S. pombe* with *nup124-1*, a defective allele of *nup124*. Using the antibody raised against Gag residues 20 to 259 (Gag$_{20-259}$), a large proportion of Gag-A5 was observed in the nucleus of the cells harvested from a log-phase culture (Fig. 12). Ninety-two percent of cells expressing Gag-A5 exhibited
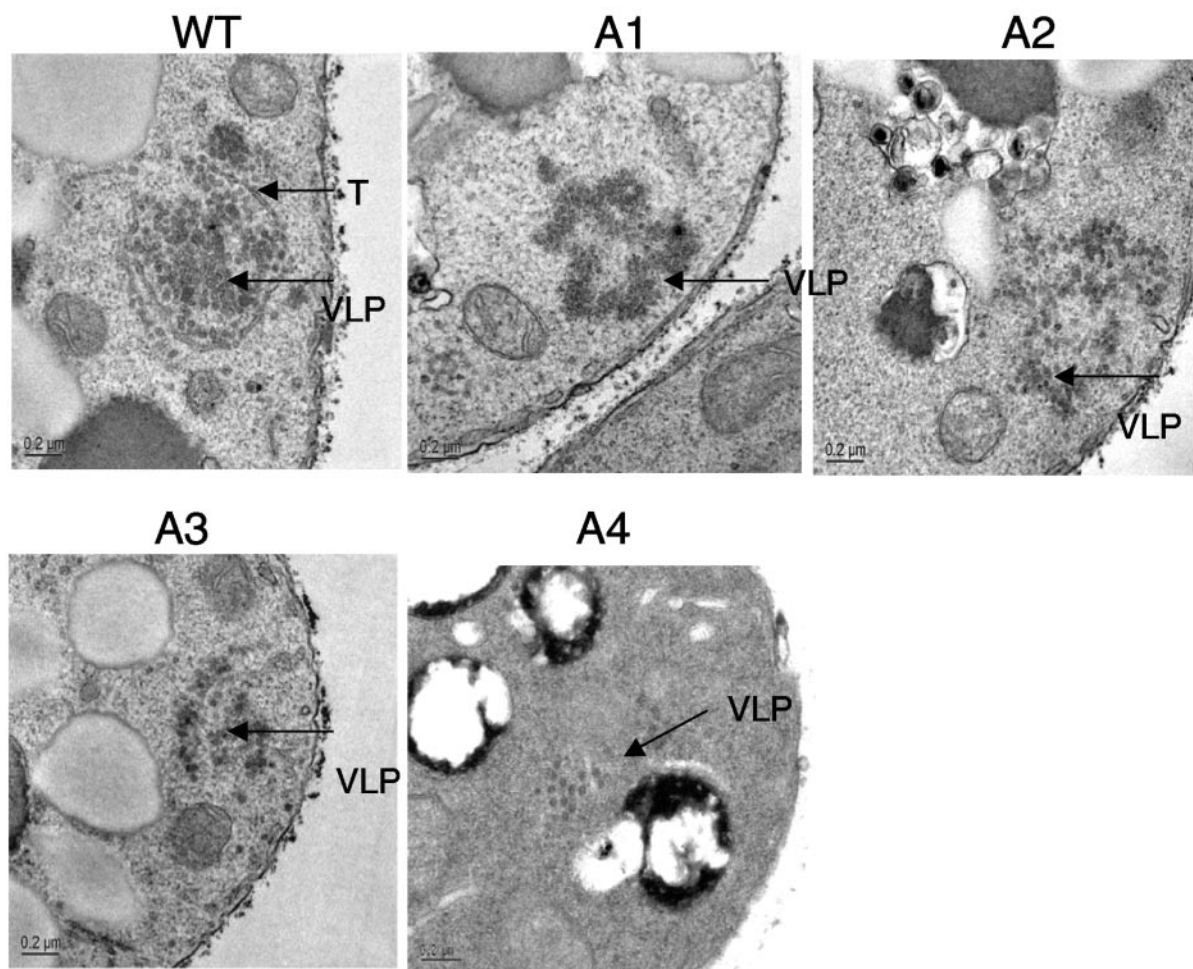
FIG. 10. The EM analysis of VLPs produced by the alanine mutants. The cells expressing WT (YHL1282), A1 (YHL8121), A2 (YHL8123), A3 (YHL8125), A4 (YHL8127), and A5 (YHL8129) were harvested from stationary phase cultures and prepared for EM examination (see Materials and Methods). These EM images were representative of >1,000 sections of cells examined for each mutant. Although >2,000 sections of cells expressing Gag-A5 were examined, no particle structures were observed. VLPs are indicated by arrows labeled VLP, and the tube-like structures from cells expressing wild-type Tf1 were indicated by a T.

strong signals of Gag associated with the nucleus. The cells expressing Gag-A4 exhibited the same interesting filaments as did the cells that were *nup124*⁺. Despite this high level of Gag organized into cytoplasmic filaments, 72% of these cells with the *nup124-1* allele showed significant concentrations of Gag associated with the nucleus (Fig. 12). These results indicate that the A4 and A5 mutations allowed nuclear localization of Gag that was independent of Nup124p.

DISCUSSION

The role of Nup124p in the localization of Gag in the nucleus is unusually specific. Nup124p is not required for the import of any of the essential proteins or any of the other proteins that were tested as reporters (6). Sedimentation experiments in sucrose gradients indicate that Gag, IN, and cDNA form a large preintegration complex (20). In this study, we found that the location of Gag in the nucleus is within the nucleolus. Together, these results indicate that the preintegration complex was localized in the nucleolus. Although there is no process of Tf1 transposition that is known to occur in the

nucleolus, it is interesting that the IN of a related LTR-containing retrotransposon, Ty3, and the proteins of several viruses concentrate in the nucleolus (12, 15, 16, 21, 28). In addition, tRNA genes are the target of integration by Ty3 and Ty1, and recent data suggest these genes are located in the nucleolus (36). In several cases, the nucleolar proteins have been found to have regulatory functions important for virus replication. This may prove to be true for the nucleolar localization of Tf1 proteins as well.

Amino acids 20 to 30 of Gag can impart the need for Nup124p on the import of a fusion protein (10). This finding led to the present study, where we asked how residues 11 to 30 contributed to the individual steps of transposition. Each of the five tracts of alanine mutations that spanned this region caused significant reductions in transposition.

To determine which mechanisms of transposition were affected by the alanine mutations, we measured the expression of Gag, the levels of full-length cDNA, and the presence of the cDNA in the nucleus. For the mutants A1, A2, and A3, the blots indicated that both Gag and cDNA levels were normal.
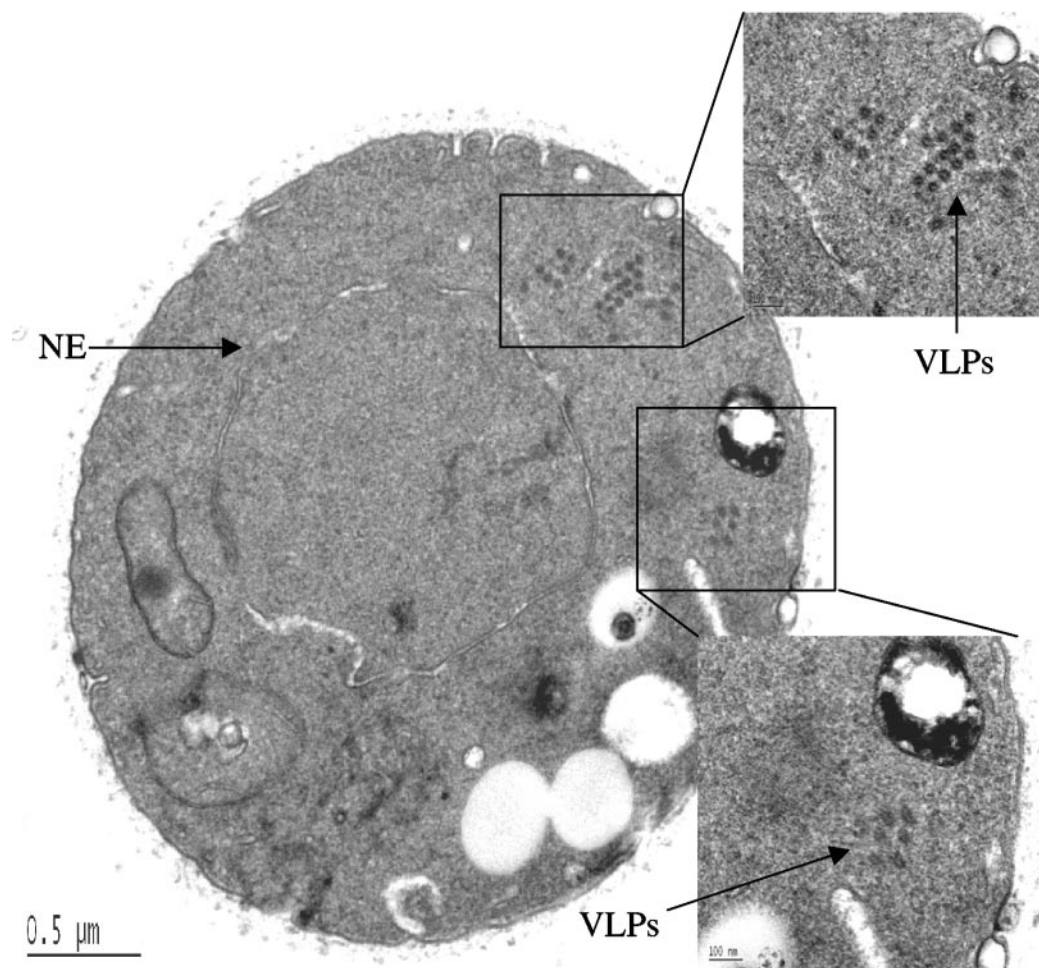
FIG. 11. EM analysis of VLPs produced by alanine mutant A4. Images of A4 particles are shown at two different magnifications, 5,000× and 20,000× (boxed area). Four distinctive patches of VLPs were observed. NE, nuclear envelope.

However, the recombination assay showed strong defects, suggesting that the cDNA was unable to enter the nucleus. The analyses of mutants A4 and A5 indicated that residues 23 through 30 had functions distinct from those of amino acids 11 through 22. Although mutant A4 produced normal levels of Gag, cDNA was absent. This indicates that residues 23 through 26 were required for reverse transcription. However, it is likely that their role in reverse transcription is an indirect result of their contribution to particle formation. Similarly, mutant A5 lacked cDNA. However, in this case the N terminus of Gag was proteolyzed as cells reached stationary phase. This makes it difficult to conclude whether these residues are required for reverse transcription. Regardless, the lack of cDNA indicates that mutants A4 and A5 disrupted transposition at an earlier step than mutants A1, A2, and A3.

The studies of nuclear localization further supported the differences between the functions of residues 11 through 22 versus 23 through 30. Mutants A1, A2, and A3 exhibited a clear defect in nuclear localization, as indicated by the immunofluorescence microscopy and the recombination assay. On the other hand, when the first 50 amino acids of Gag are fused to GFP-LacZ, only residues 1 through 10 are required for nuclear localization (10). This discrepancy underscores the difficulty of studying the import properties of short sequences by introducing them into large reporter proteins. In a single intact particle, it is estimated that there are 2,000 Gag molecules (35). As a result, the requirements for the import of Gag are likely to be more extensive than for the fusion proteins.

Although mutants A1, A2, and A3 were unable to localize in the nucleus, mutants A4 and A5 exhibited strong nuclear localization. These mutants not only allowed nuclear localization in stationary phase cells, but also had nuclear localization in log-phase cells, a condition that is restricted when Gag is wild type. It was proposed previously that a direct interaction between Nup124p, a component of the NPC, and Gag played a critical role in the import of the virus-like particles and that this was why Nup124p was specifically required for Tf1 import (6). The results of our binding experiments indicate that the first 50 amino acids of Gag do not interact with Nup124p. Thus, it is unlikely that the changes in localization of the alanine mutants were due to defects in the interaction between Nup124p and Gag. The result that each of the mutant Gags
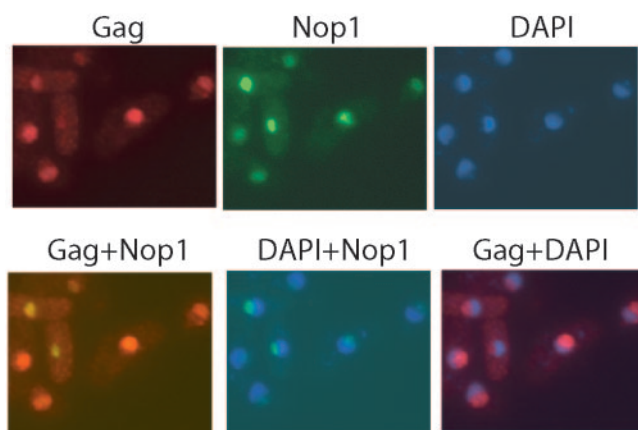
nup124-/A4
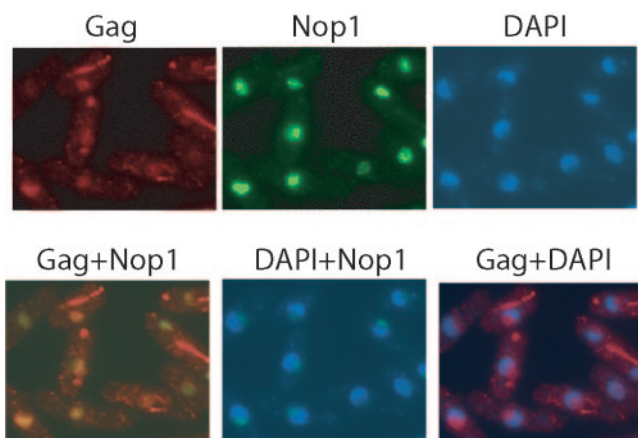
nup124-/A5

FIG. 12. The nuclear localization of Gag-A4 and Gag-A5 expressed in a strain with the *nup124-1* mutation. The antibodies used for indirect immunofluorescence were the same as those used in the results shown in Fig. 5. The cultures expressing A4 (YHL8102) and A5 (YHL8104) were harvested in log phase.

retained their ability to bind Nup124p in vitro suggests the mutations altered other processes necessary for nuclear localization.

The finding that the last 50 amino acids of Gag is the only segment that interacts with Nup124p is an important result because it will motivate experiments that test the function of this interaction in the nuclear localization of Gag. In addition, previous experiments identified two NLSs in the C terminus of Gag (10). The function of these NLSs could be due to their interaction with Nup124p.

The possibility was considered that the defects in localization and reverse transcription were due to altered structures of the mutant particles. Both differential and gradient sedimentation experiments indicated that the mutations in A1 and A2 did not significantly alter particle sedimentation. A3 exhibited normal sedimentation in the differential experiment and an

intermediate defect with gradient sedimentation, a technique that detects intact VLPs. On the other hand, A4 and A5 exhibited severe defects in both differential and gradient sedimentation experiments. The finding that A3 sedimented normally in the differential experiment was somewhat at odds with the intermediate defect seen in the sedimentation gradient. However, this difference was likely due to the presence of 1 M NaCl in the gradients, a condition that may have caused the particles of A3 to partially dissociate (39).

The examination of particle structure by EM correlated well with the data from sedimentation analyses. A1, A2, and A3, the mutants with the least changes in Gag sedimentation, did produce clusters of particles or dense aggregates, as seen with EM. A4 and A5, the mutants with the greatest defects in sedimentation either had very few particles or lacked particles altogether, as observed by EM. The finding that A1, A2, and A3 generated particles while A4 and A5 did not indicated that the defects in reverse transcription could simply be explained by the lack of particle formation. Studies of mutations in the Gags of retroviruses and retrotransposons demonstrate that particle assembly is a prerequisite for reverse transcription (33). In addition, other mutations studied in previous work indicated that Gag of Tf1 is required for reverse transcription (34). Regardless of the changes in localization associated with A4 and A5, their lack of reverse transcription was sufficient to account for their defects in transposition.

The analyses of particles also suggested explanations for the defects the alanine mutations caused in the localizations of Gag. Although mutants A1, A2, and A3 all produced particles that could be readily visualized by EM, they were poorly defined and irregular in shape (Fig. 10). This presents the possibility that the disordered particles were unable to localize in the nucleus because the NLSs in the Gag proteins were either made inaccessible or lost activity. The model that the disordered particles lost import activity was consistent with the results of EM that A1, A2, and A3 each produced at least threefold-more cell sections with cytoplasmic particles than wild-type Tf1. Although we may not know the precise cause of the cytoplasmic localization, the normal levels of protein and cDNA produced by A1, A2, and A3 indicate that their defect in transposition is primarily due to the block in nuclear access.

The severe defects of A4 and A5 in the formation of particles was particularly interesting because this loss of particles correlated with the premature localization of Gag in the nucleus, as observed by immunofluorescence microscopy. This correlation suggests a link between access to the nucleus in log phase and Gag that is unable to form particles. It is possible that mutations that disrupt the assembly of particles allow Gag to be imported by an alternative pathway. This possibility was confirmed when the Gags of A4 and A5 were both found to accumulate in the nucleus in the absence of functional Nup124p. This is in sharp contrast to wild-type Gag, which has an absolute dependence on Nup124p for nuclear localization. That the Gags of A4 and A5 localized in the nucleus much earlier in the growth of the culture than wild-type Gag also suggested that A4 and A5 used an alternative pathway independent of Nup124p. This alternative pathway of localization was not restricted in log-phase cells.

The GeneDB database of the Sanger Institute indicates that Nup124p is just one of six proteins in the NPC of *S. pombe* that

contains arrays of FG repeats. The transport receptors with their cargo proteins bind directly to the FG repeats displayed throughout the nuclear pore (1, 2, 29, 31). Currently, it is thought that transport through the pore results from an affinity gradient of FG binding sites (7, 25–27).

The change in the import pathway for the Gags of A4 and A5 that made nuclear localization independent of Nup124p may have resulted from a variety of different effects. One simple explanation is that the mutations increased the affinity of the NLS for a different transport receptor. However, this does not address the correlation between Nup124p independent import and the loss of particle formation. It is possible that individual molecules of Gag possess an alternative or cryptic NLS that becomes masked upon assembly into particles. Since the mutations block assembly of particles, the alternative NLS could be recognized by a different transport receptor than the one that recognizes intact particles. This explanation is attractive because there are now clear examples of transport receptors that interact with specific sets of FG-containing proteins in the NPC (30). Thus, an alternative transport receptor for Gag-A4 and A5 may interact with a different set of FG-containing proteins that does not include Nup124p. This type of alternate pathway might not require a direct interaction between Gag and Nup124p because in the case of A4 and A5, the transport cargo is significantly smaller than virus-like particles.

Another model for why the Gags of A4 and A5 entered the nucleus in the absence of Nup124p activity is that Nup124p may have a specific function that is only required for the import of large macromolecular cargos, such as virus-like particles. Mutant Gag that did not assemble into particles would not require Nup124p for import. The contribution of Nup124p could be associated with expanding the diameter of the pore to accommodate Tf1 particles. Currently, little is known about how cargos such as gold particles can translocate through channels of the NPC that are smaller than the particles. Another feature of large cargos that may limit translocation through the NPC may be the large numbers of NLSs in multimeric complexes. As many as 2,000 NLSs in Gag proteins are present within a single particle, and their associated transport receptors may bind in large numbers to the same NPC. Release from the NPC into the nucleoplasm of a cargo with so many independent binding sites may require a specialized mechanism. For example, Nup124p contains a large number of NLS-like sequences. These clusters of basic amino acids could be potent competitors of the NLSs in Gag and allow efficient release of Gag molecules from the transport receptors. This could result in the release of sufficient numbers of Gag molecules to allow dissociation of the particle from the NPC.

Both models that attribute the size of the cargo as restricting import imply that a direct interaction between Gag and the NPC might not be necessary in the cases of A4 and A5, because the transport cargos were significantly smaller than virus-like particles. Associated with any of the models for the function of Nup124p is the assumption that during log-phase growth, a regulatory mechanism inhibits Nup124p-dependent localization of Gag in the nucleus. The nature of this effect could be associated with regulation of the NLS or a subsequent step that regulates the activity of Nup124p.

The study of alanine mutations in the Gag of Tf1 revealed that amino acids 11 through 30 contained two subdomains that contributed different functions to transposition. Amino acids 11 through 22 are not required for particle assembly or reverse transcription. Instead they play a major role in the nuclear localization of Tf1 by supporting the function of the adjacent NLS. Amino acids 23 through 30 are required for the formation of virus-like particles and the subsequent process of reverse transcription. Although these residues are not required for nuclear localization, they play a key role in the Nup124p-dependent pathway of import. The finding that the residues 27 through 30 contribute both to particle assembly and to Nup124p-dependent import indicates that the specific requirement for Nup124p is due to extensive multimerization of Gag. It is particularly significant that the amino acids found to play a role in the Nup124p-dependent import in this study are the same amino acids found previously to cause import of GFP-LacZ to require Nup124p (10). This correlation provides additional support for the conclusion that residues 27 through 30 play an important role in the Nup124p-dependent pathway of import. Further study of Nup124p will provide important insight into how these residues contribute to the transport of large macromolecular cargos.

REFERENCES

1. **Allen, N. P. C., L. Huang, A. Burlingame, and M. Rexach.** 2001. Proteomic analysis of nucleoporin interacting proteins. J. Biol. Chem. **276:**29268–29274.
2. **Allen, N. P. C., S. S. Patel, L. Huang, R. F. Chalkley, A. Burlingame, M. Lutzmann, E. C. Hurt, and M. Rexach.** 2002. Deciphering networks of protein interactions at the nuclear pore complex. Mol. Cell. Proteomics **1:**930–946.
3. **Aris, J. P., and G. Blobel.** 1988. Identification and characterization of a yeast nucleolar protein that is similar to a rat liver nucleolar protein. J. Cell Biol. **107:**17–31.
4. **Atwood, A., J. Choi, and H. L. Levin.** 1998. The application of a homologous recombination assay revealed amino acid residues in an LTR-retrotransposon that were critical for integration. J. Virol. **72:**1324–1333.
5. **Atwood, A., J. H. Lin, and H. L. Levin.** 1996. The retrotransposon Tf1 assembles virus-like particles that contain excess Gag relative to integrase because of a regulated degradation process. Mol. Cell. Biol. **16:**338–346.
6. **Balasundaram, D., M. J. Benedik, M. Morphew, V. D. Dang, and H. L. Levin.** 1999. Nup124p is a nuclear pore factor of *Schizosaccharomyces pombe* that is important for nuclear import and activity of retrotransposon Tf1. Mol. Cell. Biol. **19:**5768–5784.
7. **Ben-Efraim, I., and L. Gerace.** 2001. Gradient of increasing affinity of importin beta for nucleoporins along the pathway of nuclear import. J. Cell Biol. **152:**411–417.
8. **Cullen, B. R.** 2001. Journey to the center of the cell. Cell **105:**697–700.
9. **Dang, V. D., M. J. Benedik, K. Ekwall, J. Choi, R. C. Allshire, and H. L. Levin.** 1999. A new member of the sin3 family of corepressors is essential for cell viability and required for retroelement propagation in fission yeast. Mol. Cell. Biol. **19:**2351–2365.
10. **Dang, V. D., and H. L. Levin.** 2000. Nuclear import of the retrotransposon Tf1 is governed by a nuclear localization signal that possesses a unique requirement for the FXFG nuclear pore factor Nup124p. Mol. Cell. Biol. **20:**7798–7812.
11. **Fouchier, R. A. M., and M. H. Malim.** 1999. Nuclear import of human immunodeficiency virus type-1 preintegration complexes, p. 275-+, Adv. Virus Res. **52:**275–299.
12. **Ginisty, H., H. Sicard, B. Roger, and P. Bouvet.** 1999. Structure and functions of nucleolin. J. Cell Sci. **112:**761–772.
13. **Goff, S. P.** 2001. Intracellular trafficking of retroviral genomes during the early phase of infection: viral exploitation of cellular pathways. J. Gene Med. **3:**517–528.
14. **Gorlich, D., and U. Kutay.** 1999. Transport between the cell nucleus and the cytoplasm. Annu. Rev. Cell Dev. Biol. **15:**607–660.

15. **Hernandez-Verdun, D., P. Roussel, and J. Gebrane-Younes.** 2002. Emerging concepts of nucleolar assembly. J. Cell Sci. **115:**2265–2270.
16. **Hiscox, J. A.** 2002. The nucleolus—a gateway to viral infection? Arch. Virol. **147:**1077–1089.
17. **Katz, R. A., J. G. Greger, P. Boimel, and A. M. Skalka.** 2003. Human immunodeficiency virus type 1 DNA nuclear import and integration are mitosis independent in cycling cells. J. Virol. **77:**13412–13417.
18. **Levin, H. L.** 1995. A novel mechanism of self-primed reverse transcription defines a new family of retroelements. Mol. Cell. Biol. **15:**3310–3317.
19. **Levin, H. L.** 1996. An unusual mechanism of self-primed reverse transcription requires the RNase H domain of reverse transcriptase to cleave an RNA duplex. Mol. Cell. Biol. **16:**5645–5654.
20. **Levin, H. L., D. C. Weaver, and J. D. Boeke.** 1993. Novel gene expression mechanism in a fission yeast retroelement: Tf1 proteins are derived from a single primary translation product. EMBO J. **12:**4885–4895. (Erratum, **13:**1494, 1994.)
21. **Lin, S. S., M. H. Nymark-McMahon, L. Yieh, and S. B. Sandmeyer.** 2001. Integrase mediates nuclear localization of Ty3. Mol. Cell. Biol. **21:**7826–7838.
22. **Losson, R., and F. Lacroute.** 1983. Plasmids carrying the yeast OMP decarboxylase structural and regulatory genes: transcription regulation in a foreign environment. Cell **32:**371–377.
23. **Moreno, S., A. Klar, and P. Nurse.** 1991. Molecular genetic analysis of fission yeast *Schizosaccharomyces pombe*. Methods Enzymol. **194:**795–823.
24. **Pante, N., and M. Kann.** 2002. Nuclear pore complex is able to transport macromolecules with diameters of similar to 39 nm. Mol. Biol. Cell **13:**425–434.
25. **Ribbeck, K., and D. Gorlich.** 2001. Kinetic analysis of translocation through nuclear pore complexes. EMBO J. **20:**1320–1330.
26. **Rout, M. P., J. D. Aitchison, M. O. Magnasco, and B. T. Chait.** 2003. Virtual gating and nuclear transport: the hole picture. Trends Cell Biol. **13:**622–628.
27. **Rout, M. P., J. D. Aitchison, A. Suprapto, K. Hjertaas, Y. M. Zhao, and B. T. Chait.** 2000. The yeast nuclear pore complex: composition, architecture, and transport mechanism. J. Cell Biol. **148:**635–651.
28. **Rowland, R. R., and D. Yoo.** 2003. Nucleolar-cytoplasmic shuttling of PRRSV nucleocapsid protein: a simple case of molecular mimicry or the complex regulation by nuclear import, nucleolar localization and nuclear export signal sequences. Virus Res. **95:**23–33.
29. **Ryan, K. J., and S. R. Wente.** 2000. The nuclear pore complex: a protein machine bridging the nucleus and cytoplasm. Curr. Opin. Cell Biol. **12:**361–371.
30. **Strawn, L. A., T. Shen, N. Shulga, D. S. Goldfarb, and S. R. Wente.** 2004. Minimal nuclear pore complexes define FG repeat domains essential for transport. Nat. Cell Biol. **6:**197–206.
31. **Strawn, L. A., T. X. Shen, and S. R. Wente.** 2001. The GLFG regions of Nup116p and Nup100p serve as binding sites for both Kap95p and Mex67p at the nuclear pore complex. J. Biol. Chem. **276:**6445–6452.
32. **Suntharalingam, M., and S. R. Wente.** 2003. Peering through the pore: nuclear pore complex structure, assembly, and function. Dev. Cell **4:**775–789.
33. **Telesnitsky, A., and S. P. Goff.** 1997. Reverse transcriptase and the generation of retroviral DNA, p. 121–160. *In* J. M. Coffin (ed.), Retroviruses. Cold Spring Harbor Laboratory Press, Cold Spring Harbor, N.Y.
34. **Teysset, L., V. D. Dang, M. K. Kim, and H. L. Levin.** 2003. A long terminal repeat-containing retrotransposon of *Schizosaccharomyces pombe* expresses a Gag-like protein that assembles into virus-like particles which mediate reverse transcription. J. Virol. **77:**5451–5463.
35. **Vogt, V. M.** 1997. Retroviral virions and genomes, p. 27–70. *In* J. M. Coffin (ed.), Retroviruses. Cold Spring Harbor Laboratory Press, Cold Spring Harbor, N.Y.
36. **Wang, L., R. A. Haeusler, P. D. Good, M. Thompson, S. Nagar, and D. R. Engelke.** 2005. Silencing near tRNA genes requires nucleolar localization. J. Biol. Chem. **280:**8637–8639.
37. **Weis, K.** 2003. Regulating access to the genome: nucleocytoplasmic transport throughout the cell cycle. Cell **112:**441–451.
38. **Yu, S. F., K. Edelmann, R. K. Strong, A. Moebes, A. Rethwilm, and M. L. Linial.** 1996. The carboxyl terminus of the human foamy virus Gag protein contains separable nucleic acid binding and nuclear transport domains. J. Virol. **70:**8255–8262.
39. **Zolotukhin, S., B. J. Byrne, E. Mason, I. Zolotukhin, M. Potter, K. Chesnut, C. Summerford, R. J. Samulski, and N. Muzyczka.** 1999. Recombinant adeno-associated virus purification using novel methods improves infectious titer and yield. Gene Ther. **6:**973–985.